

SUPPLEMENTARY MATERIAL

Authors: Alan A. Stocker (1) and Eero P. Simoncelli (2)

Affiliations: (1) Dept. of Psychology,  
University of Pennsylvania  
3401 Walnut Street 313C  
Philadelphia, PA 19104-6228  
U.S.A.

(2) Howard Hughes Medical Institute,  
Center for Neural Science and  
Courant Institute of Mathematical Sciences  
New York University  
4 Washington Place Rm 809  
New York, NY 10003-1056  
U.S.A.

Correspondence: Alan A. Stocker  
email: [astocerk@sas.upenn.edu](mailto:astocerk@sas.upenn.edu)  
phone: +1 215 573 9341

Journal: Journal of Vision

Classification: Biological Sciences (Psychology/Neuroscience)

Statistics: 8 pages, 5 figures, 0 tables

Philadelphia, May 23, 2009

# Supplementary Material

## *Extended Signature of Adaptation*

The concept of a signature of adaptation can be extended to include changes in variability of the perceptual estimate. More specifically, if we assume a gain-change model as the underlying mechanism for adaptation, and assume an appropriate noise model for the channel responses, we can predict what the characteristic change in estimation variability should be. For example, assuming the channels' responses for a given stimulus to follow a Poisson distribution, we can demonstrate with simulations that the relative change in variability of the estimate is symmetric about the adaptor, typically increased at the adaptor and decreased at adjacent values (see also [1]). Again, since the details are not important in the context of this paper, we use a simple, single-parameter function (second derivative of a Gaussian) that captures the main characteristics of the relative change in variability. Figure 1 shows the full *signature of adaptation*, for the combined changes in the mean and variability of perceptual estimates, here expressed as the difference in means ( $\mu^*(v) - \mu(v)$ ) and the relative change in standard deviation of the estimation distributions ( $\log \sigma^*(v)/\sigma(v)$ ).

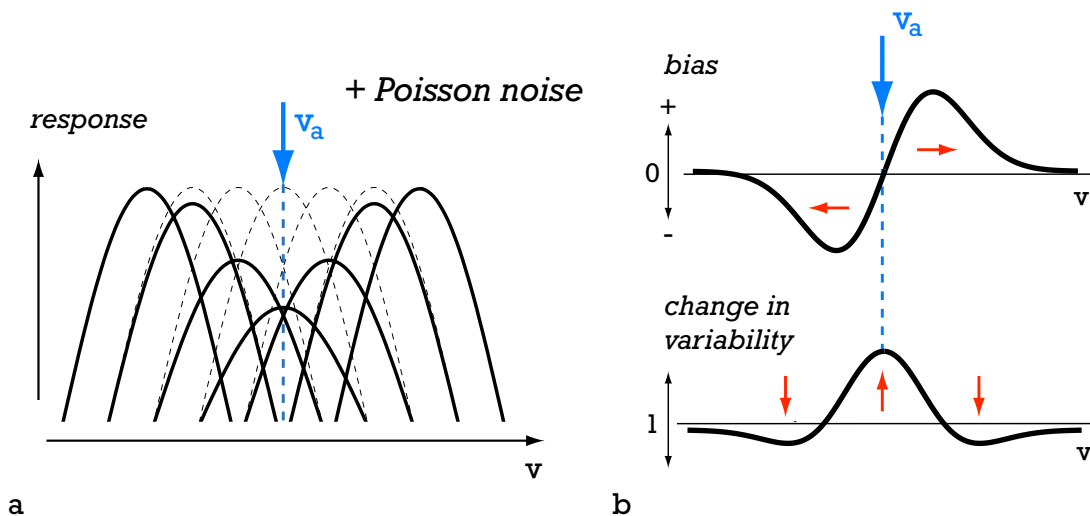


Fig. 1. *Extended signature of adaptation.* (a) The gain-change model mechanism can be extended by considering response variability [2]. (b) Decoding channel activity assuming Poisson noise statistics leads to an perceptual signature in bias *and* in change in estimation variability. The signature for variability (here expressed as the relative change of standard deviations  $\log \sigma^*(v)/\sigma(v)$ ) is symmetric around the adaptor, is increased at the adaptor and decreased for stimuli that are further away in perceptual space.

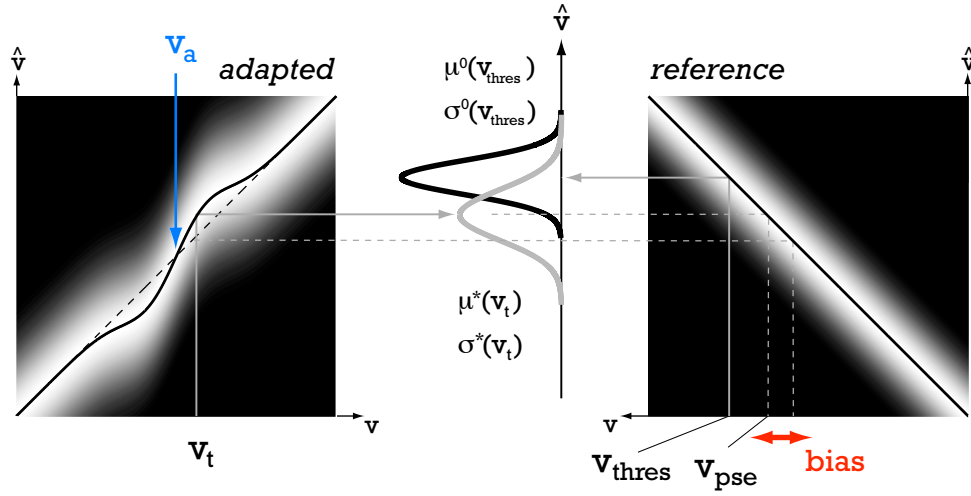


Fig. 2. *Signal detection theory and the relationship between perception and estimation.* The two gray-scale plots illustrate the distributions of a subject's estimate  $\hat{v}(v)$  under adaptation and reference conditions over a broad range of stimulus velocities  $v$ . Presumably, adaptation changes the mean  $\mu^*(v)$  as well as the standard deviation  $\sigma^*(v)$  of these distributions as a function of the adaptor  $v_a$  and the stimulus velocity  $v$ . These changes in the subjects' estimation of velocity are then expressed as changes in the point-of-subjective-equality  $v_{pse}$  and discrimination threshold  $v_{thres}$ . Signal detection theory links these perceptual measures to estimator bias ( $\mu(v)^* - \mu(v)$ ) and relative change in variability ( $\log \sigma^*(v)/\sigma(v)$ ).

#### *Linking estimation variability to perceptual 2AFC data*

While the estimation bias can be directly measured from the shift of the psychometric function under adapted versus control conditions, the changes in estimation variability are only indirectly reflected in changes in perceptual discriminability as measured by the slope of the psychometric function. This relationship is further complicated by our single-sided 2AFC adaptation protocol (see Methods in the main text). Alternatively, discriminability could have been extracted directly from a separate two-sided adaptation experiment in which both, reference and test location, were adapted. However, this would have resulted in doubling the length of the already extensive experiment because the single-sided adaptation condition is still needed to compute the bias.

In the following, we use *signal detection theory* [3], [4] to extract the changes in variability from the subjects' psychometric functions. We assume that when performing a 2AFC motion discrimination task between a reference and a test stimulus with velocities  $v_r$  and  $v_t$ , subjects perform independent estimates  $\hat{v}(v_r)$  and  $\hat{v}(v_t)$  of each stimulus velocity, and then take a decision accordingly [2]. Due to noise, these estimates will fluctuate over repeated trials, leading to distributions of estimates. By approximating the distributions of estimates

with Gaussians of mean  $\mu(v)$  and standard deviation  $\sigma(v)$ , we can define the perceptual discriminability between a reference and a test stimulus as

$$d'(v_r, v_t) = \frac{\mu(v_r) - \mu(v_t)}{\sqrt{\frac{1}{2}(\sigma^2(v_r) + \sigma^2(v_t))}}. \quad (1)$$

In general, the estimator for the test and the reference stimulus are different (see Fig.2). In our single-sided adaptation experiment, the estimator of the reference stimulus was always in the unadapted state, whereas the estimator of the test was in one of the four adaptation conditions or the control condition. For each  $v_t$  under each adaptation condition we fit the subjects' psychometric function with a cumulative Gaussian, and then extracted two values of  $v_r$  from the fit that correspond to two particular values of  $d'$ : the *point-of-subjective-equality*  $v_{\text{pse}}(v_t)$  for which  $d' = 0$ , and the *discrimination threshold velocity*  $v_{\text{thres}}(v_t)$  that is associated with a certain (arbitrarily chosen) cumulative probability  $\alpha$  on the psychometric curve (here, we use  $\alpha = 0.875$ , with an associated value of  $d'_\alpha = 1.627$ ). This is illustrated graphically in Fig.2. For each adaptation condition (fully adapted, control adapted, unadapted), Eq. (1) may be used to define these two special values of  $v_r$  through implicit equations. For example, the values  $v_{\text{pse}}^*(v_t)$  and  $v_{\text{thres}}^*(v_t)$  for the fully adapted condition are determined by

$$0 = \mu^0(v_{\text{pse}}^*(v_t)) - \mu^*(v_t) \quad (2)$$

$$d'_\alpha = \frac{\mu^0(v_{\text{thres}}^*(v_t)) - \mu^*(v_t)}{\sqrt{\frac{1}{2}((\sigma^0(v_{\text{thres}}^*(v_t))))^2 + (\sigma^*(v_t))^2}}, \quad (3)$$

for each test velocity  $v_t$  under each condition, where the superscripts  $\{*, 0\}$  indicate the adaptation state (fully adapted, and unadapted, respectively). In order to solve for  $\mu^*(v_t)$  and  $\sigma^*(v_t)$ , we make the following assumptions: (i) Without loss of generality, we assume that the estimator for the reference stimulus is veridical, *i.e.*  $\mu^0(v_r) = v_r$ . (ii) Furthermore, we also assume that the variability of the estimator changes smoothly, *i.e.* it remains roughly constant over the velocity range of the discrimination threshold.

Under assumption (i), Eq.(2) implies that  $\mu^*(v_t) = v_{\text{pse}}^*(v_t)$ . Thus, we can extract the *estimation bias* directly as the difference in the measured point-of-subjective-equality under full adaptation and control adaptation conditions:

$$\mu^*(v_t) - \mu^c(v_t) = v_{\text{pse}}^*(v_t) - v_{\text{pse}}^c(v_t).$$

We can solve for the *estimation variability*,  $\sigma^*(v_t)$ , by substituting  $v_{\text{pse}}^*(v_t)$  for  $\mu^*(v_t)$  in Eq.(3) and rewriting as

$$\sigma^*(v_t) = \frac{1}{d'_\alpha} \sqrt{2(v_{\text{thres}}^*(v_t) - v_{\text{pse}}^*(v_t))^2 - (\sigma^0(v_{\text{thres}}^*(v_t)))^2}. \quad (4)$$

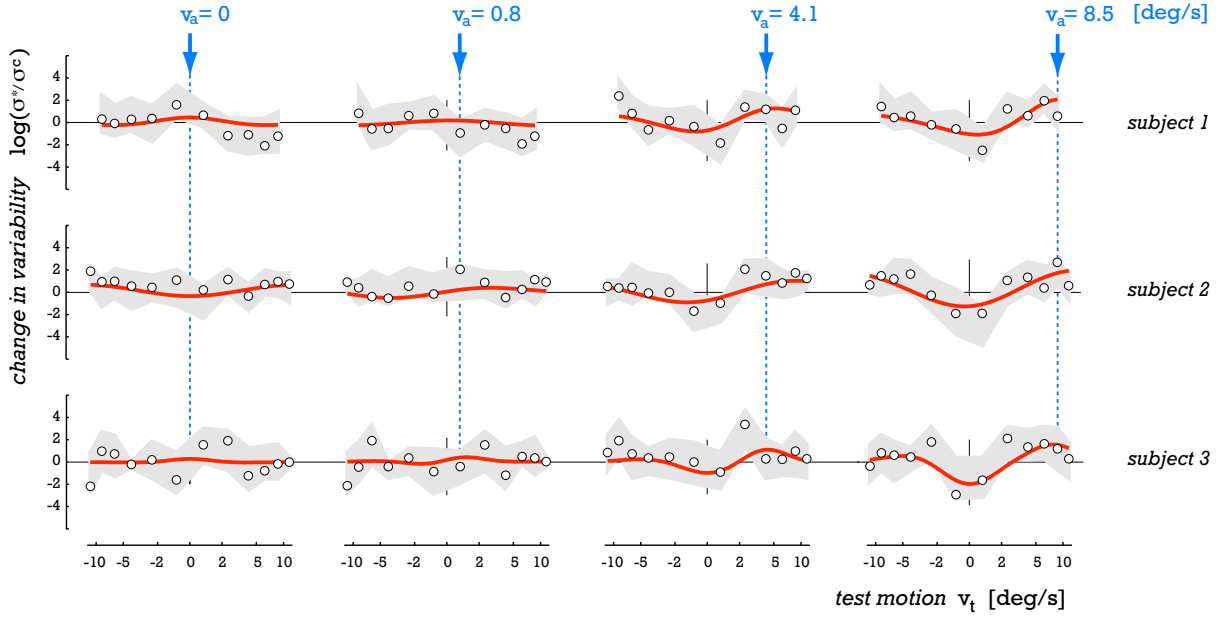


Fig. 3. *Changes in estimation variability due to adaptation.* Plotted points indicate the adaptation-induced changes in estimation variability under all adaptation conditions and all three subjects. Note, that they are not equivalent to, but rather extracted from the measured perceptual discrimination thresholds using the analysis as discussed in the text. Changes are shown as the log-ratio of the standard deviations in adaptation and control conditions. As in the case of bias, the change in variability typically increases in amplitude with increasing adaptor speeds. Bold red lines represent fits according to our model. Gray shaded area indicates the 5-95 % quantile over 1000 bootstrap samples of the data.

An analogous expression may be derived for the control condition (superscript {c}), and the two may be combined to compute the relative change in estimation variability  $\log(\sigma^*(v_t)/\sigma^c(v_t))$ .

A second control experiment measured discrimination thresholds under unadapted conditions, and provided the estimates of  $\sigma^0(v)$  that are required in Eq. (4). We assume the unadapted variability at the test location to be approximately equal to that at the reference location when evaluated at the threshold velocity:

$$\sigma^0(v_{\text{thres}}^0(v_t)) \approx \sigma^0(v_t)$$

for all  $v_t$ . Substituting this into Eq. (1), and again assuming that  $\mu^0(v) = v$  gives

$$\sigma^0(v_t) \approx \frac{v_{\text{thres}}^0(v_t) - v_t}{d'_\alpha}. \quad (5)$$

The values of  $\sigma^0(v)$  required in Eq. (4) are obtained by linear interpolation.

Figure 3 shows the adaptation-induced changes in estimation variability under all adaptation conditions and for all three subjects, extracted with above analysis. Signal detection

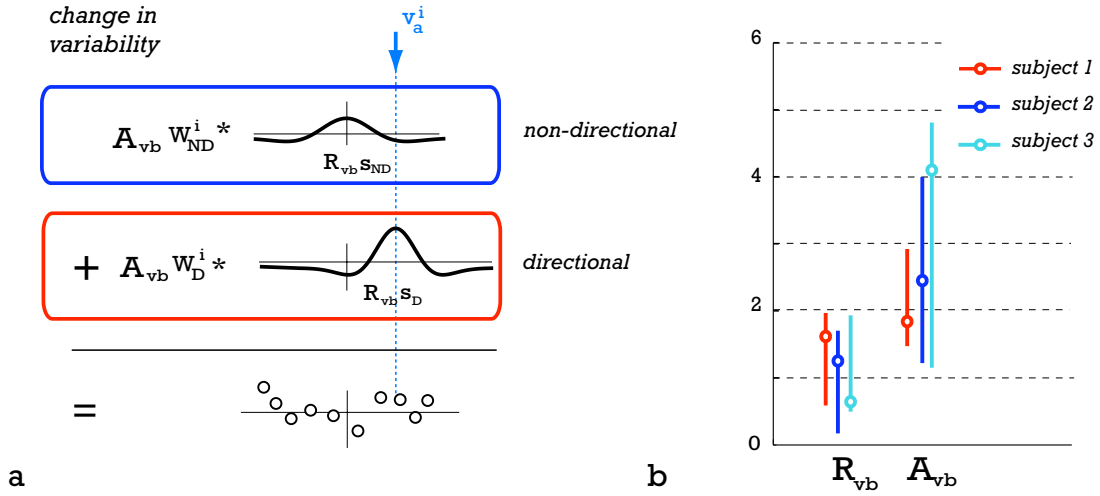


Fig. 4. *Superposition of directional and non-directional mechanism.* (a) For each subject, we used the parameter values for signature amplitudes and widths over all adaptation conditions that were fit to the estimation bias (values shown in Fig.3 in the main text). Again, the non-directional signature was centered at zero motion, while the directional signature was centered at the adaptor velocity. (b) To account for potential overall scale differences in signature width and amplitude, we allowed two extra parameters  $R_{vb}$  and  $A_{vb}$ .

theory allowed us to extract both estimation bias and changes in variability from a single one-sided adaptation experiment (see also Fig. 2), where the bias directly follows from the measured point-of-subjective-equality  $v_{\text{pse}(v_t)}$ , but the extraction of the estimation variability requires both, measurements of  $v_{\text{pse}(v_t)}$  and  $v_{\text{thres}(v_t)}$ .

#### *Model prediction and fit for changes in variability*

In order to test whether the superposition of signatures also extends to estimation variability, we predicted the expected relative changes in estimation variability based on the model parameters fit to the bias data alone (Fig.2 in main-text), and then compared this prediction to the measured variability data shown in Fig. 3. More specifically, we applied the same linear superposition of signatures as for the bias (Fig. 4), allowing only two additional parameters that account for potential scale differences in amplitude and size between the signatures for bias and relative change in variability. The fit in Fig.3 (red curves) shows that although the data are rather noisy, they are in agreement with the prediction from our model.

We have shown in previous work [5], [2], that it is important to account for both, estimation bias and variance in order to validate and constrain perceptual models with data. In this regard, it is reassuring that our hypothesis of a superposition of two isomorphic adaptation

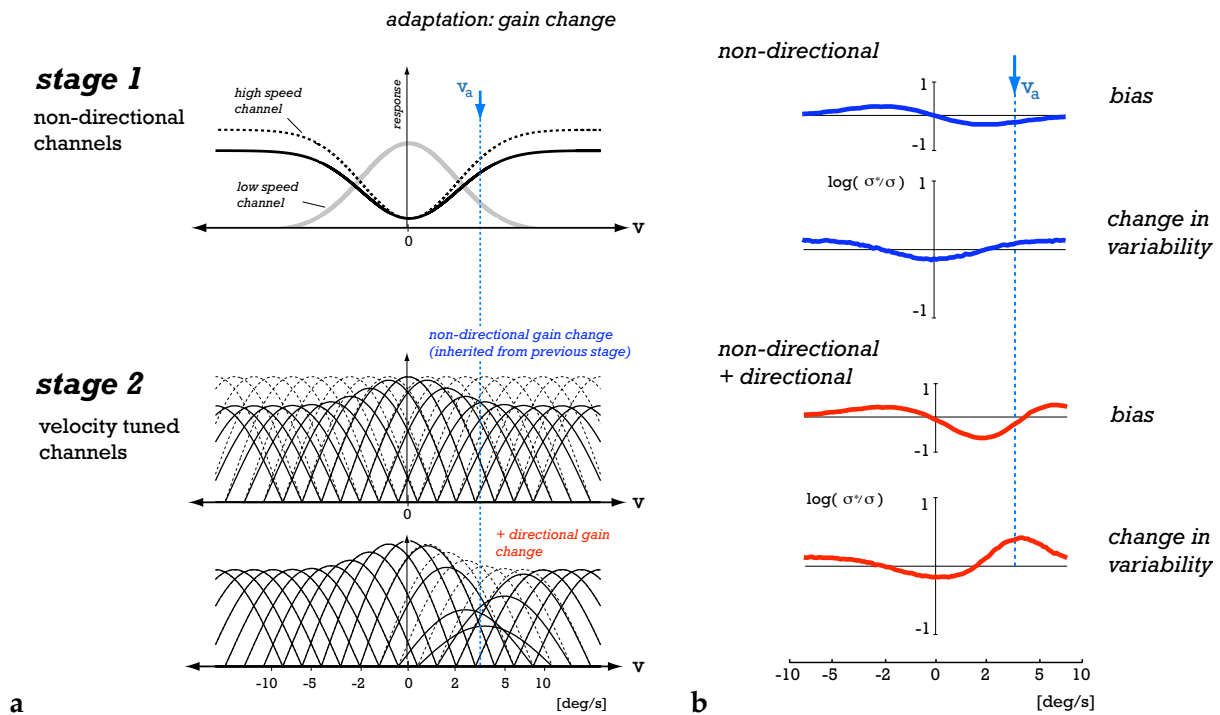


Fig. 5. *Simulated estimation variability of the cascade model.* (a) The first stage consists of two non-directional channels, tuned for low and high speeds. Adaptation changes the relative response gain of the channels based on which channel is responding more strongly to the adapting stimulus. These channels provide input to a second processing stage containing more narrowly tuned direction-selective velocity channels, which inherit the adaptation-induced gain changes of the first stage, and also undergo additional (directional) gain changes in response to the adapting stimulus. (b) Simulation results for biases and changes in variability for the case of inherited gain reduction from the first stage only (blue), as well as the full model with gain changes in both stages (red). The mean response of each channel is determined by its tuning curve (shown in (a)) and response variability was assumed to follow a Poisson process. The population response was decoded by a simple population average read-out (*i.e.*, the sum of responses, weighted by the preferred speed of each channel).

mechanisms is supported not only by the measured bias but also the changes in subjects' variabilities.

### *Simulation of the cascade model including estimation variability*

We consider the same two-stage cascade model as described in the main text, expanding it to include response variability in the channels. We assume that each channel response follows a Poisson distribution with rate determined by the associated tuning curve. As shown in Fig.5, not only bias but also estimation variability of the simulated model are in close agreement with the proposed extended signature (Fig.1).

## REFERENCES

- [1] O. Schwartz, A. Hsu, and P. Dayan. Space and time in visual context. *Nature Reviews Neuroscience*, 8:522–535, July 2007.
- [2] A.A. Stocker and E.P. Simoncelli. Noise characteristics and prior expectations in human visual speed perception. *Nature Neuroscience*, pages 578–585, April 2006.
- [3] D.M. Green and J.A. Swets. *Signal Detection Theory and Psychophysics*. Wiley, New York, 1966.
- [4] T D Wickens. *Elementary Signal Detection Theory*. Oxford University Press, 2001.
- [5] A.A. Stocker and E.P. Simoncelli. Constraining a Bayesian model of human visual speed perception. In Lawrence K. Saul, Yair Weiss, and Léon Bottou, editors, *Advances in Neural Information Processing Systems NIPS 17*, pages 1361–1368. MIT Press, Cambridge, MA, 2005.